JOINT NODE LOCALIZATION AND TIME-VARYING CLOCK SYNCHRONIZATION IN WIRELESS SENSOR NETWORKS

Aitzaz Ahmad[§], *Erchin Serpedin*[§*], *Hazem Nounou*[†], *Mohamed Nounou*[‡]

[§]Department of ECE, Texas A&M University, Texas, TX, 77843 USA.
[†]Department of ECE, Texas A&M University at Qatar, Doha, Qatar.
[‡]Department of CHEN, Texas A&M University at Qatar, Doha, Qatar.

ABSTRACT

The problems of node localization and clock synchronization in wireless sensor networks are naturally tied from a statistical signal processing perspective. In this work, we consider the joint estimation of an unknown node's location and clock parameters by incorporating the effect of imperfections in node oscillators, which render a time varying nature to the clock parameters. In order to alleviate the computational complexity associated with the optimal maximum a-posteriori estimator, a simpler approach based on the Expectation-Maximization (EM) algorithm is proposed which iteratively estimates the clock parameters using a Kalman smoother in the E-step, and the location of the unknown node in the M-step. The convergence and the mean square error (MSE) performance of the proposed algorithm are evaluated using simulation studies which demonstrate the high fidelity of the proposed joint estimation approach.

Index Terms— Node localization, clock synchronization, EM algorithm, wireless sensor networks

1. INTRODUCTION

Node localization is an important aspect of several WSN applications that require location-awareness such as geographical routing, disaster rescue, etc., [1], [2]. There is an extensive literature on location estimation algorithms in WSNs [3]. In general, the range-based localization algorithms utilize the metrics of time of arrival (TOA) [4], time difference of arrival (TDOA) [5] and received signal strength (RSS) to determine the distance between the unknown node and the anchors. Clock synchronization in sensor networks is a critical component in data fusion and duty cycling operations, and has gained widespread interest in recent years [6]. Several algorithms have been proposed for the estimation of clock parameters under different network delay distributions [7], [8], [9], [10]. Since TOA and TDOA are time-based techniques, clock synchronization is an important prerequisite in node localization [11]. This connection between the problems of localization and synchronization necessitates a joint estimation approach [12]. Recently, several contributions have studied joint localization and synchronization from a statistical signal processing viewpoint. Optimal and sub-optimal algorithms for estimating an unknown node's position and clock parameters have been derived and compared with the Cramér-Rao lower bound (CRB) in [13]. A weighted least squares approach for joint estimation is devised in [14]. Robust joint estimation algorithms resistant to target node's uncertainties are derived in [15]. However, a common theme in these contributions is the assumption of *fixed* clock parameters.

Sensor nodes are often deployed in harsh environmental conditions which can degrade the quartz crystals over time. Failure to cope with temporal variations can result in frequent re-synchronization requests. Since power is primarily consumed in radio transmission delivering timing information [16], exchanging time-stamps for re-synchronization can quickly drain a sensor's energy resources. In this work, we aim to introduce the notion of temporal variation in clock parameters for joint node localization and clock synchronization in WSNs. We develop an iterative estimation approach based on the Expectation-Maximization (EM) algorithm which simplifies the otherwise computationally costly maximum a-posteriori (MAP) estimator.

2. SYSTEM MODEL

The unknown node X, located at $\boldsymbol{x} = [x_1, x_2]^T$, communicates with the j^{th} anchor node using a two-way message exchange mechanism as shown in Fig. 1. At the k^{th} message exchange, Node X transmits its current timing information to the anchor through time-stamp $S_{j,k}$. The anchor records the time $R_{j,k}$ at at which this message is received according to its own time scale. The j^{th} anchor replies at time $\bar{S}_{j,k}$ and transmits a synchronization packet containing both the time-stamps $R_{j,k}$ and $\bar{S}_{j,k}$ to Node X. This message is received at time $\bar{R}_{j,k}$ by Node X according to its own clock. Therefore, after K exchanges with the j^{th} anchor, Node X is equipped with time-stamps $\left\{S_{j,k}, R_{j,k}, \bar{S}_{j,k}, \bar{R}_{j,k}\right\}_{k=1}^{K}$. In this work, it is assumed that the clock of Node X is related to the reference time t at each anchor node as $C_X(t) = \alpha t + \beta$, where α

*The work of E. Serpedin was supported in part by NSF grant 0915444.

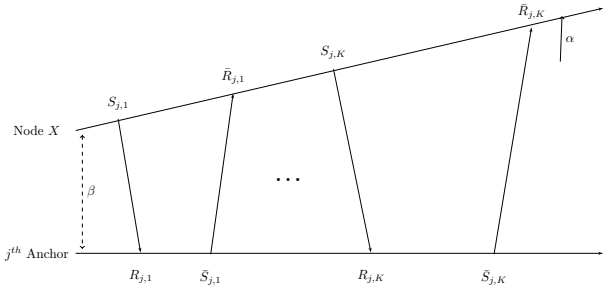

Fig. 1. A two-way timing message exchange mechanism

and β denote the clock skew and clock offset with respect to the reference time, respectively. Hence, the aforementioned two-way timing exchange process can be expressed as [17]

$$\begin{aligned} S_{j,k} &= \alpha\left(R_{j,k} - d_j - w_{j,k}\right) + \beta \\ \bar{R}_{j,k} &= \alpha\left(\bar{S}_{j,k} + d_j + \bar{w}_{j,k}\right) + \beta\,, \end{aligned} \tag{1}$$

where the measurement noise errors $w_{j,k}$ and $\bar{w}_{j,k}$ are assumed *i.i.d.* Gaussian with zero mean and variance σ_w^2. The *fixed* line-of-sight propagation delay, denoted by d_j, is given by[1] $d_j = \|\boldsymbol{x} - \boldsymbol{s}_j\|$. By defining $\theta_1 \triangleq \frac{1}{\alpha}$ and $\theta_2 \triangleq \frac{\beta}{\alpha}$, we can equivalently express (1) as

$$\boldsymbol{y}_k - \boldsymbol{d}\left(\boldsymbol{x}\right) = \boldsymbol{H}_k\boldsymbol{\theta} + \boldsymbol{w}_k\,, \tag{2}$$

where $\boldsymbol{y}_k$=$\left[R_{1,k}, -\bar{S}_{1,k}, \ldots, R_{N,k}, -\bar{S}_{N,k}\right]^T$, the parameter vector $\boldsymbol{\theta} \triangleq [\theta_1\ \theta_2]^T$, $\boldsymbol{w}_k = [w_{1,k}, \bar{w}_{1,k}, \ldots, w_{N,k}, \bar{w}_{N,k}]$, $\boldsymbol{d}\left(\boldsymbol{x}\right) = \left[d_1\mathbf{1}_{2\times1}^T, \ldots, d_N\mathbf{1}_{2\times1}^T\right]^T$, and the $2N \times 2$ matrix $\boldsymbol{H}_k$ is given by

$$\boldsymbol{H}_k = \begin{bmatrix} S_{1,k} & -1 \\ -\bar{R}_{1,k} & 1 \\ \vdots & \vdots \\ S_{N,k} & -1 \\ -\bar{R}_{N,k} & 1 \end{bmatrix}\,.$$

Since sensor nodes are usually deployed in harsh environmental conditions, degradations in quartz oscillators render a time-varying nature to the clock skew and offset of Node X. In this work, it is assumed that the variations in the clock parameters induce a Gauss-Markov evolution model for $\boldsymbol{\theta}$ at the k^{th} message exchange, i.e.,

$$\boldsymbol{\theta}_k = \boldsymbol{\theta}_{k-1} + \boldsymbol{n}_k\,, \tag{3}$$

where $\boldsymbol{n}_k$ is *i.i.d* zero mean Gaussian noise with covariance matrix $\boldsymbol{P}_n = \sigma_n^2\boldsymbol{I}$. This model helps to capture time variations and also lends mathematical simplicity to gain a theoretical insight into the problem of joint localization and time-varying clock synchronization. Using (3), the two-way message exchange model (2) at the k^{th} round is now expressed as

$$\boldsymbol{y}_k - \boldsymbol{d}\left(\boldsymbol{x}\right) = \boldsymbol{H}_k\boldsymbol{\theta}_k + \boldsymbol{w}_k\,. \tag{4}$$

The joint distribution of $\boldsymbol{y} = \left[\boldsymbol{y}_1^T, \ldots, \boldsymbol{y}_K^T\right]^T$ and $\boldsymbol{\Theta} = \left[\boldsymbol{\theta}_1^T, \ldots, \boldsymbol{\theta}_K^T\right]^T$, parameterized by $\boldsymbol{x}$, can be expressed as

$$\begin{aligned} f(\boldsymbol{y}, \boldsymbol{\Theta}; \boldsymbol{x}) &= f\left(\boldsymbol{\Theta}\right) f\left(\boldsymbol{y}|\boldsymbol{\Theta}; \boldsymbol{x}\right) \\ &= f\left(\boldsymbol{\theta}_0\right) \prod_{k=1}^{K} f\left(\boldsymbol{\theta}_k|\boldsymbol{\theta}_{k-1}\right) \prod_{k=1}^{K} f\left(\boldsymbol{y}_k|\boldsymbol{\theta}_k; \boldsymbol{x}\right)\,. \end{aligned} \tag{5}$$

The pdfs $f\left(\boldsymbol{\theta}_k|\boldsymbol{\theta}_{k-1}\right)$ and $f\left(\boldsymbol{y}_k|\boldsymbol{\theta}_k; \boldsymbol{x}\right)$ are given by

$$f\left(\boldsymbol{\theta}_k|\boldsymbol{\theta}_{k-1}\right) = C_1 \exp\left(-\frac{\left(\boldsymbol{\theta}_k - \boldsymbol{\theta}_{k-1}\right)^T\left(\boldsymbol{\theta}_k - \boldsymbol{\theta}_{k-1}\right)}{2\sigma_n^2}\right)$$

$$f\left(\boldsymbol{y}_k|\boldsymbol{\theta}_k; \boldsymbol{x}\right) =$$

$$C_2 \exp\left(-\frac{\left(\boldsymbol{y}_k - \boldsymbol{d}\left(\boldsymbol{x}\right) - \boldsymbol{H}_k\boldsymbol{\theta}_k\right)^T\left(\boldsymbol{y}_k - \boldsymbol{d}\left(\boldsymbol{x}\right) - \boldsymbol{H}_k\boldsymbol{\theta}_k\right)}{2\sigma_w^2}\right)$$

where C_1 and C_2 are constants. Our goal is to jointly estimate $\boldsymbol{\xi} = \left[\boldsymbol{\Theta}^T, \boldsymbol{x}^T\right]^T$ using the time-stamps as well as the known anchor locations $\boldsymbol{s}_j$, for $j = 1, \ldots, N$.

The joint estimates of $\boldsymbol{\Theta}$ and $\boldsymbol{x}$ can be obtained as

$$\left\{\hat{\boldsymbol{\Theta}}, \hat{\boldsymbol{x}}\right\} = \arg\max_{\boldsymbol{\Theta}, \boldsymbol{x}} \ln f(\boldsymbol{y}, \boldsymbol{\Theta}; \boldsymbol{x})\,. \tag{6}$$

Solving (6) requires inverting large matrices which is computationally demanding. In the next section, a simpler iterative approach based on the EM algorithm is explored for joint localization and timing synchronization.

3. THE EM ALGORITHM

Assuming that the data $\boldsymbol{y}$ is incomplete, the complete data vector is defined as $\boldsymbol{z} \triangleq \left[\boldsymbol{y}^T, \boldsymbol{\Theta}^T\right]^T$. The expectation and maximization steps in the EM algorithm can be described as follows [18].

E-Step:
Given an estimate $\hat{\boldsymbol{x}}^{(i)}$ of the unknown node's location at iteration i, and the observed data $\boldsymbol{y}$, determine the likelihood function

$$Q\left(\boldsymbol{x}, \hat{\boldsymbol{x}}^{(i)}\right) \triangleq \mathbb{E}_{\boldsymbol{\Theta}|\boldsymbol{y}, \hat{\boldsymbol{x}}^{(i)}}\left[\ln f\left(\boldsymbol{z}; \boldsymbol{x}\right)\right]\,. \tag{7}$$

M-Step:
Obtain an estimate of $\boldsymbol{x}$ at iteration index $i+1$ by maximizing $Q\left(\boldsymbol{x}, \hat{\boldsymbol{x}}^{(i)}\right)$, i.e.,

$$\hat{\boldsymbol{x}}^{(i+1)} = \arg\max_{\boldsymbol{x}} Q\left(\boldsymbol{x}, \hat{\boldsymbol{x}}^{(i)}\right)\,. \tag{8}$$

The E-Step and M-Step are repeated until convergence. After each iteration, we are guaranteed to converge towards a local maximum [18].

[1]The speed of light constant c is omitted for brevity.

Using (5), it follows that

$$\ln f(\boldsymbol{z};\boldsymbol{x}) = C - \frac{1}{2\sigma_w^2}\sum_{k=1}^{K}\left(\tilde{\boldsymbol{y}}_k(\boldsymbol{x}) - \boldsymbol{H}_k\boldsymbol{\theta}_k\right)^T\left(\tilde{\boldsymbol{y}}_k(\boldsymbol{x}) - \boldsymbol{H}_k\boldsymbol{\theta}_k\right) \tag{9}$$

where $\tilde{\boldsymbol{y}}_k(\boldsymbol{x}) \triangleq \boldsymbol{y}_k - \boldsymbol{d}(\boldsymbol{x})$ and the terms that do not depend on $\boldsymbol{x}$ are collected in the constant C . The likelihood function at the i^{th} iteration, $Q\left(\boldsymbol{x}, \hat{\boldsymbol{x}}^{(i)}\right)$, can be evaluated as

$$\begin{aligned} &Q\left(\boldsymbol{x}, \hat{\boldsymbol{x}}^{(i)}\right) = \\ &\mathbb{E}_{\boldsymbol{\Theta}|\boldsymbol{y},\hat{\boldsymbol{x}}^{(i)}}\left[-\frac{1}{2\sigma_w^2}\sum_{k=1}^{K}\left(\tilde{\boldsymbol{y}}_k(\boldsymbol{x}) - \boldsymbol{H}_k\boldsymbol{\theta}_k\right)^T\left(\tilde{\boldsymbol{y}}_k(\boldsymbol{x}) - \boldsymbol{H}_k\boldsymbol{\theta}_k\right)\right] \\ &= -\frac{1}{2\sigma_w^2}\sum_{k=1}^{K}\mathrm{Tr}\Bigg\{\mathbb{E}_{\boldsymbol{\Theta}|\boldsymbol{y},\hat{\boldsymbol{x}}^{(i)}}\Bigg[\left(\tilde{\boldsymbol{y}}_k(\boldsymbol{x}) - \boldsymbol{H}_k\boldsymbol{\theta}_k\right)\cdot \\ &\qquad\qquad \left(\tilde{\boldsymbol{y}}_k(\boldsymbol{x}) - \boldsymbol{H}_k\boldsymbol{\theta}_k\right)^T\Bigg]\Bigg\}. \end{aligned} \tag{10}$$

By defining

$$\hat{\boldsymbol{\theta}}_{k|K}^{(i)} \triangleq \mathbb{E}_{\boldsymbol{\Theta}|\boldsymbol{y},\hat{\boldsymbol{x}}^{(i)}}\left[\boldsymbol{\theta}_k\right], \quad \hat{\boldsymbol{R}}_{k|K}^{(i)} \triangleq \mathbb{E}_{\boldsymbol{\Theta}|\boldsymbol{y},\hat{\boldsymbol{x}}^{(i)}}\left[\boldsymbol{\theta}_k\boldsymbol{\theta}_k^T\right],$$

the likelihood function in (10) can be expressed as

$$\begin{aligned} Q\left(\boldsymbol{x}, \hat{\boldsymbol{x}}^{(i)}\right) = \frac{-1}{2\sigma_w^2}\sum_{k=1}^{K}\mathrm{Tr}\Big\{&\tilde{\boldsymbol{y}}_k(\boldsymbol{x})\,\tilde{\boldsymbol{y}}_k^T(\boldsymbol{x}) + \boldsymbol{H}_k\hat{\boldsymbol{R}}_{k|K}^{(i)}\boldsymbol{H}_k^T \\ &-\tilde{\boldsymbol{y}}_k(\boldsymbol{x})\,\hat{\boldsymbol{\theta}}_{k|K}^{(i)^T}\boldsymbol{H}_k^T - \boldsymbol{H}_k\hat{\boldsymbol{\theta}}_{k|K}^{(i)}\tilde{\boldsymbol{y}}_k^T(\boldsymbol{x})\Big\}. \end{aligned} \tag{11}$$

After some algebraic steps, (11) can be equivalently written as

$$\begin{aligned} Q\left(\boldsymbol{x}, \hat{\boldsymbol{x}}^{(i)}\right) = -\frac{1}{2\sigma_w^2}\sum_{k=1}^{K}\mathrm{Tr}\Bigg\{&\boldsymbol{H}_k\hat{\boldsymbol{\Sigma}}_{k|K}^{(i)}\boldsymbol{H}_k^T \\ &+\left(\tilde{\boldsymbol{y}}_k(\boldsymbol{x}) - \boldsymbol{H}_k\hat{\boldsymbol{\theta}}_{k|K}^{(i)}\right)\left(\tilde{\boldsymbol{y}}_k(\boldsymbol{x}) - \boldsymbol{H}_k\hat{\boldsymbol{\theta}}_{k|K}^{(i)}\right)^T\Bigg\} \end{aligned} \tag{12}$$

where

$$\hat{\boldsymbol{\Sigma}}_{k|K}^{(i)} \triangleq \hat{\boldsymbol{R}}_{k|K}^{(i)} - \hat{\boldsymbol{\theta}}_{k|K}^{(i)}\hat{\boldsymbol{\theta}}_{k|K}^{(i)^T}.$$

Given an estimate $\hat{\boldsymbol{x}}^{(i)}$, it can be observed that (3) and (4) represent a linear Gaussian model. The minimum mean square error (MMSE) estimator $\hat{\boldsymbol{\theta}}_{k|K}^{(i)}$ can be obtained from a standard Kalman smoother. The forward recursion for obtaining $\hat{\boldsymbol{\theta}}_{k|k}^{(i)}$ can be expressed as follows [19].

Forward Recursion

Prediction:

$$\begin{aligned} \hat{\boldsymbol{\theta}}_{k|k-1}^{(i)} &= \hat{\boldsymbol{\theta}}_{k-1|k-1}^{(i)} \\ \hat{\boldsymbol{\Sigma}}_{k|k-1}^{(i)} &= \hat{\boldsymbol{\Sigma}}_{k-1|k-1}^{(i)} + \sigma_n^2\boldsymbol{I} \end{aligned} \tag{13}$$

Correction:

$$\begin{aligned} \boldsymbol{\kappa}_k &= \hat{\boldsymbol{\Sigma}}_{k|k-1}^{(i)}\boldsymbol{H}_k^T\left(\boldsymbol{H}_k\hat{\boldsymbol{\Sigma}}_{k|k-1}^{(i)}\boldsymbol{H}_k^T + \sigma_w^2\boldsymbol{I}\right) \\ \hat{\boldsymbol{\theta}}_{k|k}^{(i)} &= \hat{\boldsymbol{\theta}}_{k|k-1}^{(i)} + \boldsymbol{\kappa}_k\left(\tilde{\boldsymbol{y}}_k\left(\hat{\boldsymbol{x}}^{(i)}\right) - \boldsymbol{H}_k\hat{\boldsymbol{\theta}}_{k|k-1}^{(i)}\right) \\ \hat{\boldsymbol{\Sigma}}_{k|k}^{(i)} &= \left(\boldsymbol{I} - \boldsymbol{\kappa}_k\boldsymbol{H}_k\right)\hat{\boldsymbol{\Sigma}}_{k|k-1}^{(i)} \end{aligned} \tag{14}$$

The operation of a smoother is completed by employing a backward sweep that produces the smoothed estimates $\hat{\boldsymbol{\theta}}_{k|K}^{(i)}$ and $\hat{\boldsymbol{\Sigma}}_{k|K}^{(i)}$. The recursions of the Rauch-Tung-Striebel (RTS) smoother are given as follows [20].

Backward Recursion

$$\begin{aligned} \boldsymbol{B}_{k-1} &= \hat{\boldsymbol{\Sigma}}_{k-1|k-1}^{(i)}\hat{\boldsymbol{\Sigma}}_{k|k-1}^{(i)^{-1}} \\ \hat{\boldsymbol{\theta}}_{k-1|K}^{(i)} &= \hat{\boldsymbol{\theta}}_{k-1|k-1}^{(i)} + \boldsymbol{B}_{k-1}\left(\hat{\boldsymbol{\theta}}_{k|K}^{(i)} - \hat{\boldsymbol{\theta}}_{k|k-1}^{(i)}\right) \\ \hat{\boldsymbol{\Sigma}}_{k-1|K}^{(i)} &= \hat{\boldsymbol{\Sigma}}_{k-1|k-1}^{(i)} + \boldsymbol{B}_{k-1}\left(\hat{\boldsymbol{\Sigma}}_{k|K}^{(i)} - \hat{\boldsymbol{\Sigma}}_{k|k-1}^{(i)}\right)\boldsymbol{B}_{k-1}^T. \end{aligned} \tag{15}$$

Using $\hat{\boldsymbol{\theta}}_{k|K}^{(i)}$, the estimates of $\boldsymbol{\alpha}$ and $\boldsymbol{\beta}$ can, in turn, be obtained by using the transformation in defined in Section 2. The resulting estimates are sub-optimal since, in general, the MAP estimator does not commute over non-linear transformations. However, the sub-optimal estimators show good fidelity performance as shown in Section 4.

The M-step can now be expressed using (8) as

$$\begin{aligned} \hat{\boldsymbol{x}}^{(i+1)} = \arg\max_{\boldsymbol{x}}\frac{-1}{2\sigma_w^2}\sum_{k=1}^{K}\mathrm{Tr}\Big\{&\boldsymbol{H}_k\hat{\boldsymbol{\Sigma}}_{k|K}^{(i)}\boldsymbol{H}_k^T \\ &+\left(\tilde{\boldsymbol{y}}_k(\boldsymbol{x}) - \boldsymbol{H}_k\hat{\boldsymbol{\theta}}_{k|K}^{(i)}\right)\left(\tilde{\boldsymbol{y}}_k(\boldsymbol{x}) - \boldsymbol{H}_k\hat{\boldsymbol{\theta}}_{k|K}^{(i)}\right)^T\Big\}. \end{aligned}$$

After some simplifications, the estimate $\hat{\boldsymbol{x}}^{(i+1)}$ is given as the solution of a 2-D norm minimization problem

$$\hat{\boldsymbol{x}}^{(i+1)} = \arg\min_{\boldsymbol{x}}\sum_{k=1}^{K}\left\|\tilde{\boldsymbol{y}}_k(\boldsymbol{x}) - \boldsymbol{H}_k\hat{\boldsymbol{\theta}}_{k|K}^{(i)}\right\|^2. \tag{16}$$

A closed form solution of the aforementioned minimization problem does not exist. The interior point methods can be used to obtain the estimates $\hat{\boldsymbol{x}}^{(i+1)}$ [21].

The EM algorithm, therefore, provides estimates of $\boldsymbol{\Theta}$ and $\boldsymbol{x}$ by alternating between the E and M-steps, respectively. The algorithm is terminated when the sequence $\hat{\boldsymbol{x}}^{(1)}, \hat{\boldsymbol{x}}^{(2)}, \hat{\boldsymbol{x}}^{(3)}, \ldots$ converges.

4. SIMULATION RESULTS

This section presents simulation results to evaluate the convergence and MSE performance of the proposed EM algorithm. The clock skew and offset are drawn randomly from

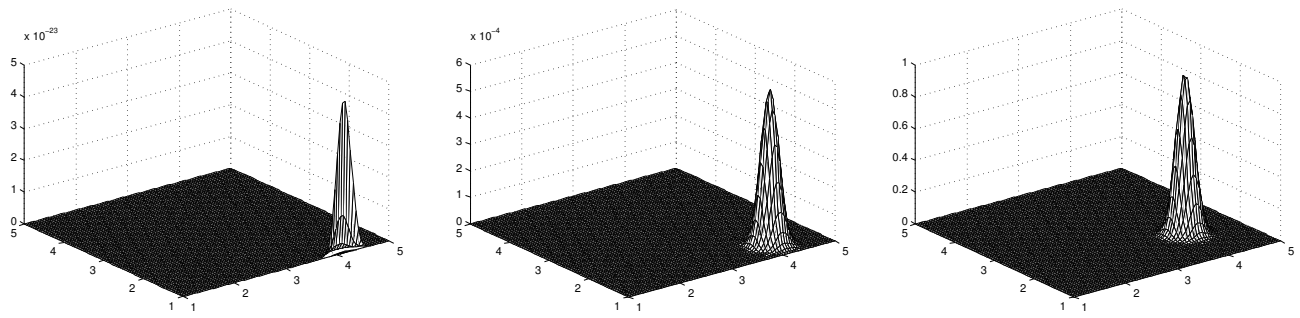

Fig. 2. The updates of $\exp\left(Q\left(\boldsymbol{x}, \hat{\boldsymbol{x}}^{(i)}\right)\right)$ versus the number of iterations i for $i = 1$, $i = 4$ and $i = 12$ with number of message exchanges $K = 2$ and measurement noise variance $\sigma_w^2 = 10^{-1}$.

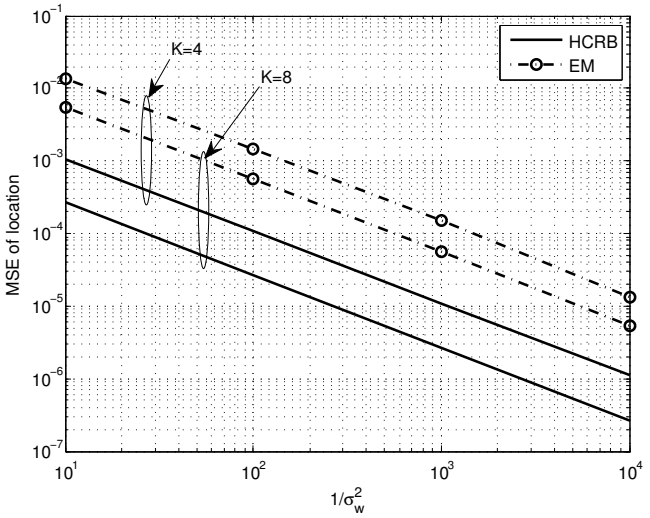

Fig. 3. A comparison of MSE of location estimates versus measurement noise variance σ_w^2 for $K = 4$ and $K = 8$.

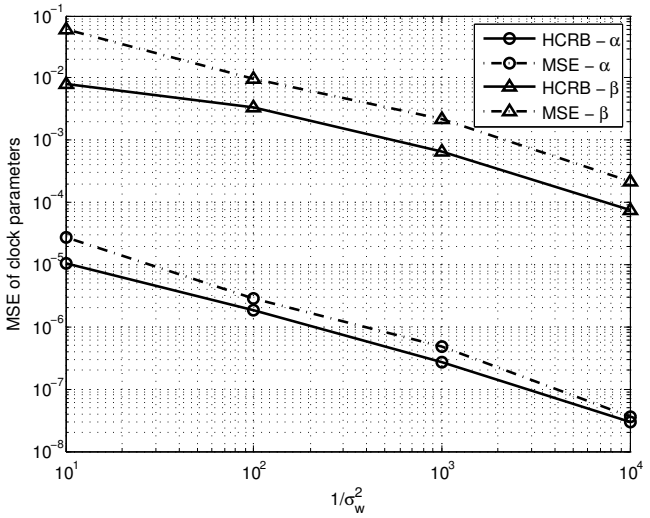

Fig. 4. A comparison of MSE of skew estimates versus measurement noise variance σ_w^2 for $K = 4$.

$[0.998, 1.002]$ and $[1, 10]$, respectively. Unless stated otherwise, the location of Node X is generated by drawing x_1 and x_2 randomly from $[1, 10]$.

In order to show the updates in the EM algorithm, the simulation results are averaged over 100 realizations of $\boldsymbol{x} = (2, 4)$ with $\sigma_w^2 = 10^{-1}$ and $K = 2$. Fig. 2 shows the updates in the likelihood function $\exp\left(Q\left(\boldsymbol{x}, \hat{\boldsymbol{x}}^{(i)}\right)\right)$ as a function of $\boldsymbol{x}$ as i increases. Clearly, $\exp\left(Q\left(\boldsymbol{x}, \hat{\boldsymbol{x}}^{(i)}\right)\right)$ is a concave function and hence, does not present any local maxima. This allows the algorithm to converge at the solution uniquely.

Fig. 3 illustrates the MSE of the location estimate as σ_w^2 decreases. The MSE decays with a decrease in σ_w^2 and the decay increases as K increases from $K = 4$ to $K = 8$. In addition, the MSE remains fairly close to the theoretical hybrid Cramer-Rao bound (HCRB), derived in [22], but does not attain it. This could potentially be due to the reason that HCRB is known to be less tight for the non-random part of the parameters [23]. The MSE of the skew and offset estimates provided by the EM algorithm is illustrated in Fig. 4 as the measurement noise decreases. It is observed that the proposed estimator has high fidelity and matches closely with the lower bound provided by HCRB. It can also be noticed that the MSE incurred in estimating clock offset is higher than the corresponding values for clock skew.

5. CONCLUSIONS

In this work, joint localization and time-varying clock synchronization of an unknown node is considered. An iterative approach using the EM algorithm is proposed which iteratively estimates the unknown node's location by considering the clock parameters as hidden variables. Simulation results corroborate our theoretical findings and demonstrate the high accuracy of the proposed EM algorithm.

6. REFERENCES

[1] S. Gezici, "A survey on wireless position estimation," *Wireless Personal Communications(Special Issue on Towards Global and Seamless Personal Navigation)*, vol. 44, no. 3, pp. 263–282, Feb. 2008.

[2] S. Gezici, Z. Tian, G. Giannakis, H. Kobayashi, A. Molisch, H. Poor, and Z. Sahinoglu, "Localization via ultra-wideband radios: A look at positioning aspects for future sensor networks," *Signal Processing Magazine, IEEE*, vol. 22, no. 4, pp. 70 – 84, Jul. 2005.

[3] A. H. Sayed, A. Tarighat, and N. Khajehnouri, "Network-based wireless location: Challenges faced in developing techniques for accurate wireless location information," *IEEE Signal Processing Mag.*, vol. 22, no. 4, pp. 24–40, Jul. 2005.

[4] K. W. Cheung, H. C. So, W.-K. Ma, and Y. T. Chan, "Least squares algorithms for time-of-arrival-based mobile location," *IEEE Transactions on Signal Processing*, vol. 52, no. 4, pp. 1121–1130, Apr. 2004.

[5] Y. Huang, J. Benesty, G. W. Elko, and R. M. Mersereati, "Real-time passive source localization: A practical linear-correction least-squares approach," *IEEE Transactions on Speech and Audio Processing*, vol. 9, no. 8, pp. 943–956, Nov. 2001.

[6] E. Serpedin and Q. Chaudhari, *Synchronization in Wireless Sensor Networks: Parameter Estimation, Performance Benchmarks, and Protocols*. Cambridge University Press, 2009.

[7] H. Abdel-Ghaffar, "Analysis of synchronization algorithms with time-out control over networks with exponentially symmetric delays," *IEEE Transactions on Communications*, vol. 50, no. 10, pp. 1652–1661, Oct. 2002.

[8] D. Jeske, "On maximum-likelihood estimation of clock offset," *IEEE Transactions on Communications*, vol. 53, no. 1, pp. 53–54, Jan. 2005.

[9] K.-L. Noh, Q. Chaudhari, E. Serpedin, and B. Suter, "Novel clock phase offset and skew estimation using two-way timing message exchanges for wireless sensor networks," *IEEE Transactions on Communications*, vol. 55, no. 4, pp. 766 –777, Apr. 2007.

[10] Q. Chaudhari, E. Serpedin, and K. Qaraqe, "Some improved and generalized estimation schemes for clock synchronization of listening nodes in wireless sensor networks," *Communications, IEEE Transactions on*, vol. 58, no. 1, pp. 63–67, Jan. 2010.

[11] R. Poovendran, C. Wang, and S. Roy, *Secure Localization and Time Synchronization for Wireless Sensor and ad hoc networks*. New York; Springer, 2006.

[12] Y.-C. Wu, Q. Chaudhari, and E. Serpedin, "Clock synchronization of wireless sensor networks," *IEEE Signal Processing Magazine*, vol. 28, no. 1, pp. 124–138, Jan. 2011.

[13] J. Zheng and Y.-C. Wu, "Joint time synchronization and localization of an unknown node in wireless sensor networks," *IEEE Transactions on Signal Processing*, vol. 58, no. 3, pp. 1309–1320, Mar. 2010.

[14] S. Zhu and Z. Ding, "Joint synchronization and localization using TOAs: A linearization based approach," *IEEE J. Sel. Areas Commun.*, vol. 28, no. 7, pp. 1017–1025, Sep. 2010.

[15] Y. Wang, X. Ma, and G. Leus, "Robust time-based localization for asynchronous networks." *IEEE Transactions on Signal Processing*, vol. 59, no. 9, pp. 4397–4410, Sep. 2011.

[16] G. J. Pottie, W. J. Kaiser, M. Giona, and S. Barbarossa, "Wireless integrated network sensors," *Commun., ACM*, vol. 43, no. 5, pp. 51–58, May 2000.

[17] Q. Chaudhari, E. Serpedin, and K. Qaraqe, "On maximum likelihood estimation of clock offset and skew in networks with exponential delays," *IEEE Transactions on Signal Processing*, vol. 56, no. 4, pp. 1685–1697, Apr. 2008.

[18] A. P. Dempster, N. M. Laird, and D. B. Rubin, "Maximum likelihood from incomplete data via the EM algorithm," *Journal of the Royal Statistical Society*, vol. 39, Series B, pp. 1–38, 1977.

[19] S. M. Kay, *Fundamentals of Statistical Signal Processing. Estimation Theory*. Prentice-Hall, 1993.

[20] H. E. Rauch, F. Tung, and C. T. Striebel, "Maximum likelihood estimates of linear dynamic systems," *AIAA Journal*, vol. 3, no. 8, pp. 1445–1450, Aug. 1965.

[21] Y. Nesterov and A. Nemirovskii, *Interior-Point Polynomial Algorithms in Convex Programming*. SIAM, 1994.

[22] A. Ahmad, E. Serpedin, H. Nounou, and M. Nounou, "Joint node localization and time-varying clock synchronization in wireless sensor networks," *submitted to IEEE Transactions on Wireless Communications*.

[23] H. Messer, "The Hybrid Cramér-Rao bound - From practice to theory," in *IEEE workshop on Sensors, Array and Multichannel Signal Process.*, 2006.